

## **Original Research Article**

### **Some Molecular Properties and Reaction Mechanism of Synthesized Isatin Thiosemicarbazone and Its Zinc(II) and Nickel(II) Complexes**

**Abstract:** The aim of this study is to 1H-Indole-2,3-dione 3-[N-(4-fluorophenyl)-thiosemicarbazone and its zinc(II) and nickel(II) complexes. The structures of the synthesized compounds were confirmed by spectral data and elemental analysis. They were optimized by B3LYP theory with different basis sets. The optimized structures were compared with the experimental values. TD-DFT calculations on electronic absorption spectra in gas phase and DMSO were performed to determine the electronic transitions of the compounds. The Frontier Molecular Orbital analysis were also done in order to identify the charge transfer interaction that takes place between the molecular orbitals. Reaction mechanism of 1H-indole-2,3-dione-3-(N-4-fluorophenyl thiosemicarbazone) molecules were also studied.

**Keywords:** Isatin; metal complexes; thiosemicarbazone; chemical computational calculations

#### **1. INTRODUCTION**

Isatin thiosemicarbazones are the most important class of biologically active ligands providing potential binding sites through nitrogen and sulphur donor atoms belong to thiosemicarbazone group and oxygen donor atoms belong to indole ring [1-5]. Metal complexes of isatin thiosemicarbazone derivatives, especially Zn(II), Ni(II), Pd(II) and Pt(II), have been extensively synthesized by several researchers because of their biological active properties, such as antibacterial, antiviral, anti-tuberculosis, antifungal activities [6-11].

We have recently experimentally synthesized and characterized some isatin thiosemicarbazones complexes, such as 5-methoxy and 5-fluoro isatin thiosemicarbazone, and theoretically studied the quantum chemical properties [12-18].

In this study, the theoretical vibrational spectrum, UV spectrum,  $^{13}\text{C}$  and  $^1\text{H}$  NMR values, molecular polarizability, molecular geometry, and atomic charges have been performed for 3-(N-4-fluorophenyl)-1H-indole-2,3-dione thiosemicarbazone and its zinc(II) and nickel(II) complexes by using B3LYP hybrid functional with basis sets, 6-31G(d,p), 6-311G(d,p), 6-311++G(d,p) and

6-311++G(2d,2p). Fukui functions have been calculated by using AOMix [16-17] from single-point calculations with B3LYP/6-311G(d,p).

## 2. MATERIAL AND METHOD

### 2.1. Experimental

Synthesis of 1H-indole-2,3-dione 3-[N-(4-fluorophenyl)-thiosemicarbazone-I4FPTH<sub>2</sub>] was carried out by stirring 0.294 g (2 mmol) of isatin in 75 mL ethanol on a hot plate magnetic stirrer until dissolved and adding 0.306 g (2 mmol) of 4-fluorophenyl-3-thiosemicarbazide dissolved in ethanol and about 2-3 drops of fuming sulphuric acid on isatin solution under stirring, respectively. The mixture was refluxed for about 2-3 hours. The precipitated product was filtered, purified and dried. Orange solid product was obtained.

C<sub>15</sub>H<sub>11</sub>ON<sub>4</sub>S (Melting point, MP: 240.9 °C and Molecule weight, MW= 314.34 g/mol), IR(cm<sup>-1</sup>): 3293, 3174(NH), 1684(C=O), 1621(C=N), 867(C=S), <sup>1</sup>H NMR(DMSO-d<sub>6</sub>,ppm): 7.74(dd, 1H, indol-C<sub>4</sub>-H), 7.58(dd, 2H, phenyl), 7.35(dt, 1H, indol-C<sub>5</sub>-H), 7.27(dd, 2H, phenyl), 7.13(dt, 1H, indol-C<sub>6</sub>-H), 6.92(dd, 1H, indol-C<sub>7</sub>-H), 10.83(t, 1H, N<sub>4</sub>-H), 11.26(s, 1H, indol-NH), 12.80(s, 1H, N<sub>2</sub>-H), (Calc.: C, 57.31; H, 3.53; N, 17.82; S, 10.20%; Found: C, 55.78; H, 2.96; N, 17.43; S, 10.93%).

#### 2.1.1. Synthesis of bis{1H-indole-2,3-dione 3-[N-(4-fluorophenyl)thiosemicarbazonato}Zn(II) - Zn[(I4FPTH)<sub>2</sub>]

0.3142 g (1 mmol) of I4FPTH<sub>2</sub> was dissolved in 20 mL methanol at about 50-55 °C and then 0.1097 g (0.5 mmol) of zinc acetate tetra hydrate dissolved in 15 mL methanol was slowly added on it to synthesize the Zn[(I4FPTH)<sub>2</sub>] complex. The mixture was refluxed for about 6-9 hours. A dark orange product was obtained. The Zn[(I4FPTH)<sub>2</sub>] complex was washed with ethanol and diethyl ether, and then dried (MP: 256 °C). (Calc.: C, 52.07; H, 2.91; N, 16.19; S, 8.98%; Found: C, 51.66; H, 2.92; N, 15.91; S, 8.98%).

#### 2.1.2. Synthesis of bis{1H-indole-2,3-dione 3-[N-(4-fluorophenyl)thiosemicarbazonato}Ni(II) Ni[(I4FPTH)<sub>2</sub>]

Ni[(I4FPTH)<sub>2</sub>] complex was synthesized by dissolving 0.3142 g (1 mmol) of I4FPTH<sub>2</sub> in 20 mL of methanol at about 50-55 °C and then slowly adding 15 mL methanol solution containing 0.1244 g (0.5 mmol) of nickel acetate tetrahydrate. The mixture was refluxed for about 2 hours. Brown

Ni[(I4FPTH)<sub>2</sub>] complex was precipitated, washed with ethanol and diethyl ether, and then dried (MP: 258 °C). (Calc.: C, 52.57; H, 2.94; N, 15.91; S, 9.35%; Found: C, 50.94; H, 2.90; N, 15.60; S, 8.67%).

## 2.2. Calculation Method

I4FPTH<sub>2</sub> ligand was optimized at the level of B3LYP theory with 6-31G(d,p), 6-311G(d,p), 6-311++G(d,p), 6-311G(2d,2p) basis sets, and Zn[(I4FPTH)<sub>2</sub>], Ni[(I4FPTH)<sub>2</sub>] complexes were optimized at the level of B3LYP theory with 6-31G(d,p), 6-311G(d,p) basis sets in gas phase and DMSO solvent. <sup>1</sup>H and <sup>13</sup>C NMR chemical shifts were calculated by using the GIAO method at the level of B3LYP theory with 6-31G(d,p), 6-311G(d,p), 6-311++G(d,p), 6-311G(2d,2p) basis sets for I4FPTH<sub>2</sub> ligand. Reaction mechanism of I4FPTH<sub>2</sub> ligand was performed with semi-empirical method by using AM1 Package program. Gaussian 09 was used to perform calculations [19].

## 3. Result and Discussion

Figure 1 shows the optimized structure of 1H-indole-2,3-dione 3-[N-(4-fluorophenyl)-thiosemicarbazone molecules with the atom numbering calculated by using B3LYP/6-311G(d,p). Calculated bond lengths of I4FPTH<sub>2</sub> molecule with B3LYP/6-31G(d,p), B3LYP/6-311G(d,p), B3LYP/6-311++G(d,p), B3LYP/6-311G(2d,2p) method in gas phase and DMSO solvent are given in Figure 2 and Mulliken charges are presented in Figure 3.

It was observed that there was negative charges density on C17, C11, C5, C4, N6, O9, N21, N20, S7, N19 atoms in both gas and liquid (DMSO) phase. Calculations were completed by using B3LYP method and 6-31G(d,p), 6-311G(d,p), 6-311++G(d,p), 6-311G(2d,2p) basis sets for I4FPTH<sub>2</sub>. Charge densities vary in accordance with the basis sets and depending on whether the gas or liquid phases. Mulliken charge of C17 atom calculated with the 6-31G(d,p), 6-311G(d,p), 6-311++G(d,p), 6-311G(2d,2p) basis sets are -0.125, -0.027, -0.330, -0.302 ē, respectively in gas phase, while in DMSO are -0.148, -0.051, -0.351, -0.315 ē and for N21 atom in gas phase are -0.380, -0.240, -0.068, -0.373 ē while in DMSO -0.386, -0.241, -0.082, -0.396 ē.

The optimized structures for the Zn[(I4FPTH)<sub>2</sub>] and Ni[(I4FPTH)<sub>2</sub>] calculated with B3LYP/6-311G(d,p) level are given in Figure 4. Bond lengths calculated with the B3LYP level and 6-311G(d,p) 6-31G(d,p), 6-311G(d,p) basis sets are given in Figure 5 and Mulliken charges are given in Figure 6. As can be seen from the Figure 5, there is no significant difference in bond lengths according to the basis sets. Therefore, either 6-311G(d,p), or 6-311G(d,p) basis sets might be preferred to calculate bond lengths.

Bond lengths of I4FPTH<sub>2</sub> ligand, Zn[(I4FPTH)<sub>2</sub>] and Ni[(I4FPTH)<sub>2</sub>] complexes calculated according to B3LYP/6-311G(d,p) theory are given in Figure 7. Bond length for C15-C17 atoms belong to indole ring for I4FPTH<sub>2</sub> ligand, Zn[(I4FPTH)<sub>2</sub>] and Ni[(I4FPTH)<sub>2</sub>] complexes is 1.390, 1.393, 1.395 Å; for C10-N6 bond length is 1.403, 1.396, 1.392 Å; for C18-N21 bond length is 1.296, 1.305, 1.310 Å and for N21-N20 bond length is 1.332, 1.357, 1.347 Å, respectively. There is a little increasing in bond lengths at thiosemicarbazone side of complexes.

Negative charge density on C11, C5, C4, N6, O9 atoms and positive charge density on C10, C12, C18 atoms belong to indole ring of Zn[(I4FPTH)<sub>2</sub>] complex was found. The negative charge density on C11, C5, C4, N6, O9 atoms are -0.106 ē, -0.092, -0.108 ē, -0.674 ē, -0.476 ē, for 6-31G(d,p) basis set and 0.034, -0.135, -0.083, -0.048, -0.490, -0.316 ē, for 6-311G(d,p) basis set, respectively. The positive charge density on C10, C12, C18 atoms are 0.304, 0.622, 0.261 ē; for 6-31G(d,p) basis set and 0.252, 0.429, 0.204 ē for 6-311G(d,p) basis set, respectively. N21, N20, S7, N19 atoms belong to thiosemicarbazone group have negative charge density, these are 0.499, -0.308, -0.227, -0.598 ē for 6-31G(d,p) basis set, and -0.533, -0.220, -0.436, -0.399 ē for 6-311G(d,p) basis set, respectively. Mulliken charge calculated with 6-311G(d,p) is lower than of 6-31G(d,p).

According to B3LYP/6-311G(d,p) theory; the Mulliken charges on C17, C11, C5, C4, C10, C15, N6, C12, O9, C18 atoms are -0.027, -0.100, -0.090, -0.041, 0.239, -0.135, -0.489, 0.422 ē, for I4FPTH<sub>2</sub> ligand; 0.034, -0.135, -0.083, -0.048, 0.252, -0.157, -0.490, 0.429, -0.316, 0.204 ē, for Zn[(I4FPTH)<sub>2</sub>] complex and 0.012, -0.113, -0.082, -0.051, 0.239, -0.132, -0.488, 0.312, -0.322, 0.224 ē, for Ni[(I4FPTH)<sub>2</sub>] complex, respectively. Mulliken charges on N21, N20, C16, S7, N19, C13 belong to thiosemicarbazone group are -0.240, -0.270, 0.230, -0.214, -0.462, 0.199 ē, for I4FPTH<sub>2</sub> ligand; -0.533, -0.220, 0.164, -0.436, -0.399, 0.143 ē, for Zn[(I4FPTH)<sub>2</sub>] complex and -0.485, -0.263, 0.195, -0.312, -0.428, 0.169 ē, for Ni[(I4FPTH)<sub>2</sub>] complex, respectively. Mulliken charge of Zn atom in Zn[(I4FPTH)<sub>2</sub>] complex and Ni atom in Ni[(I4FPTH)<sub>2</sub>] complex were calculated as 1.379 and 1.045 ē (Figure 8).

### 3.1 Reaction mechanism study of 1H-indole-2,3-dione-3-(N-4-fluorophenyl thiosemicarbazone) molecules

The calculation was carried out on protonated form of 1H-indole-2,3-dione and 4-(4-Fluorophenyl)-3-thiosemicarbazide and continued to protonated form of product in the reaction mechanism study. The reaction mechanism was studied with semi-empirical method Austin Model (AM1). Reactants, transition states (TS), intermediates (IN1) and products of spatial arrangements of atoms are given in Figure 9. Bond lengths and Mulliken charges of 1a-2, TS1, IN1, TS2, 3b molecules are given in Figure 10.

Gaussian assumes electronic distribution as a function of the molecular geometry (Born-Oppenheimer approximation). The vibrational frequency calculations are required for understanding whether it has been obtained from a stable minimum structure. Negative imaginary frequencies were found in calculations for TS1 and TS2 (the negative frequencies for TS1 and TS2 are 315 and 1743  $\text{cm}^{-1}$ ).

As well as the presence of a negative frequency defining the minima connected through the transition state is required. We chose the intrinsic reaction coordinate (IRC), and defined as the minimum energy reaction pathway (MERP) in mass-weighted Cartesian coordinates that between the transition state of a reaction and its reactants and products (Figure 11).

4-(4-Fluorophenyl)-3-thiosemicarbazide molecule and protonated 1H-indole-2,3-dione molecule are far from each other ( $\text{C13-N17} = 3.00 \text{ \AA}$ ). The distance between N17 atom belong to 34-(4-Fluorophenyl)-3-thiosemicarbazide molecule and C13 atom attached to protonated 1H-indole-2,3-dione molecule in the transition state, intermediate state and product state is 1.950, 1.496, 1.560, 1.314  $\text{\AA}$ , respectively. C=O bond length belong to indole ring in reactant state, TS1, IN, TS2 and product state is found as 1.226, 1.229, 1.230, 1.232 and 1.226  $\text{\AA}$ , respectively. The Mulliken charge of N17 atom in reactant state, TS1, IN, TS2 and product state is 0.290, -0.235, -0.001, -0.052, -0.025  $e$ , respectively and the Mulliken charge of C11 atom in reactant state is 0.276, 0.299, 0.144, 0.107, 0.144  $e$ , respectively. This explains that, N17 atom belong to 4-(4-Fluorophenyl)-3-thiosemicarbazide molecule attacks to C13 atom attached to protonated 1H-indole-2,3-dione ring as nucleophile.

The reactivity of a molecule is closely related to the highest occupied molecular orbital-HOMO and the lowest empty molecular orbital -LUMO and the parameters such as hardness, softness can be calculated using HOMO and LUMO energies. The higher value of  $E_{\text{HOMO}}$  means its ability to donate electrons to appropriate acceptor molecules with low energy empty MO.  $E_{\text{HOMO}}$  value indicates the ability to donate electrons and  $E_{\text{LUMO}}$  indicates the ability to accept electrons. HOMO, LUMO energies and five molecular orbital energies close to HOMO and LUMO of I4FPTH<sub>2</sub> molecule obtained from the calculations with the 6-31G(d,p), 6-311G(d, p), 6-311++G(d,p), 6-311G(2d,2p) basis sets of B3LYP method in gas phase and solvent (DMSO) (Figure 12) and those for  $\text{Zn}[(\text{I4FPTH})_2]$ ,  $\text{Ni}[(\text{I4FPTH})_2]$  calculated with the 6-31G(d,p), 6-311G(d,p) basis sets of B3LYP method are given in Figure 13.

It was observed that  $E_{\text{HOMO}}$  and  $E_{\text{LUMO}}$  values calculated with B3LYP method for carried out basis sets in DMSO solvent were lower than those in gas phase. For example, while  $E_{\text{HOMO}}$  values in the gas phase calculations by using 6-31G(d,p), 6-311G(d,p), 6-311++G(d,p), 6-311G(2d,2p) basis sets are -0.21723, -0.22651, -0.23083, -0.22967 au, in the DMSO solvent calculations are -

0.22080, -0.22847, -0.23206, -0.23073 au.  $E_{\text{LUMO}}$  values are -0.09713, -0.10535, -0.11099, -0.10979 au in gas phase, and -0.09283, -0.10157, -0.10648, -0.10528 au in DMSO solvent.

HOMO and LUMO energies for  $\text{Zn}[(\text{I4FPTH})_2]$ ,  $\text{Ni}[(\text{I4FPTH})_2]$  calculated with 6-31G(d,p) basis set is higher than those calculated with 6-311G(d,p) basis set. HOMO with the 5 molecular orbital energies close to Frontier orbitals and LUMO with the 5 molecular orbital energies close to Frontier orbitals are -0.20833, -0.20901, -0.21880, -0.22292, -0.23609, -0.23976, -0.10223, -0.10212, -0.01653, -0.01576, -0.00909, -0.00879 au for the calculations with 6-31G(d,p) basis set and are 0.21823, -0.21868, -0.22907, -0.23242, -0.24647, -0.24876, -0.11209, -0.11104, -0.02777, -0.02744, -0.02112, -0.02102 au for the calculations with 6-311G(d,p) basis set (Figure 13).

Frontier orbital energies of ligand and its zinc(II) and nickel(II) complexes are given in Figure 14. HOMO energy for I4FPTH<sub>2</sub> ligand and  $\text{Zn}[(\text{I4FPTH})_2]$ ,  $\text{Ni}[(\text{I4FPTH})_2]$  complexes at the level of theory B3LYP/6-311G(d,p) were calculated as -0.22651, 0.19795, -0.21823 au, respectively and LUMO energies of those were calculated as -0.10535, -0.10037, -0.11209 au. HOMO energies of complexes are higher than its ligand.

The electronic energy data for I4FPTH<sub>2</sub> calculated with 6-311G(d,p), 6-311++G(d,p), 6-311++G(2d,2p) basis sets in gas phase and DMSO solvent and for  $\text{Zn}[(\text{I4FPTH})_2]$ ,  $\text{Ni}[(\text{I4FPTH})_2]$  complexes calculated with 6-31G(d,p), 6-311G(d,p) basis sets are given in Table 1 in au units.

The electronic energy for I4FPTH<sub>2</sub> calculated with the level of B3LYP/6-31G(d,p), B3LYP/6-311G(d,p), B3LYP/6-311++G(d,p), B3LYP/6-311++G(2d,2p) are -1370.50690942, -1370.75982233, -1370.77771190, -1370.81055509 au, respectively. The lowest electronic energy structure was predicted by B3LYP/6-311++G(2d,2p) in DMSO solvent. Calculated electronic energies in DMSO (-1370.83735522 au) is lower than in gas phase (-1370.81055509 au) for the same basis sets.

Polarizability,  $\alpha$ , is the distortion outer electrons under the influence of the electric field as a result of migration from one region to another in the presence of an electric field. As  $\alpha$  increase, electron cloud can be polarized easily. Electric dipole polarization may be calculated by the following equation.

$$\alpha = \frac{1}{3}(\alpha_{xx} + \alpha_{yy} + \alpha_{zz})$$

Polarizability increases when basis set level increases. Polarizability values calculated with 6-31G(d,p), 6-311G(d,p), 6-311++G(d,p), 6-311++G(2d,2p) basic sets of B3LYP theory for I4FPTH<sub>2</sub> ligand are 246.4, 257.0, 277.5, 283.0 Bohr<sup>3</sup>, respectively. The polarizability of metal complexes is more than their ligands (Table 2).

### 3.2. NMR Study

$^1\text{H}$  and  $^{13}\text{C}$  NMR values for I4FPTH<sub>2</sub> ligand calculated with 6-31G(d,p), 6-311G(d,p), 6-311++G(d,p), 6-311G(2d,2p) basis sets of B3LYP theory in gas phase and DMSO solvent are given in Tables 3 and 4 with the experimental values.  $^1\text{H}$  and  $^{13}\text{C}$  NMR values of Zn[(I4FPTH)<sub>2</sub>] complex calculated with 6-31G(d,p) and 6-311G(d,p) basis sets with the experimental ones are presented in Table 5.

The correlation coefficient excluding Hydrogen atom belonging to indole ring in  $^1\text{H}$  NMR calculations performed with B3LYP and 6-31G(d,p), 6-311G(d,p), 6-311++G(d,p), 6-311G(2d,2p) basis sets in gas phase is found as 0.856, 0.861, 0.864, 0.888 ppm, respectively and in DMSO solvent 0.773, 0.841, 0.870, 0.870 ppm, respectively (Table 3).

The correlation coefficient of  $^{13}\text{C}$  NMR calculations performed with B3LYP and 6-31G(d,p), 6-311G(d,p), 6-311++G(d,p), 6-311G(2d,2p) basis sets in gas phase is found as 0.987, 0.984, 0.984, 0.985 ppm, respectively and in DMSO solvent 0.950, 0.941, 0.983, 0.985 ppm, respectively. Correlation coefficients between calculated and observed chemical shifts for  $^{13}\text{C}$  NMR carried out with B3LYP and 6-31G(d,p), 6-311G(d,p), 6-311++G(d,p), 6-311G(2d,2p) basis sets are 0.987, 0.984, 0.984, 0.985 ppm, respectively in DMSO solvent and are in 0.950, 0.941, 0.983, 0.985 ppm in gas phase (Table 4). Accordingly,  $^1\text{H}$  NMR calculation performed with B3LYP/6-311G(2d,2p) calculation in DMSO gives excellent correlation between computed and observed  $^{13}\text{C}$  NMR spectra.

The lack of N-H31 chemical shift belong to thiosemicarbazone group for Zn[(I4FPTH)<sub>2</sub>] complex which is observed for I4FPTH<sub>2</sub> ligand indicates that deprotonation take place during complexation reaction.

### 3.3. UV Study

UV calculations for molecular structure of I4FPTH<sub>2</sub> ligand, Zn[(I4FPTH)<sub>2</sub>] and Ni[(I4FPTH)<sub>2</sub>] were simulated by using TDDFT. Oscillator strengths (f) and excitation energies (eV) for UV spectra values of all studied compounds were summarized in Table 6 with the experimental values.

176th molecular orbital calculated with B3LYP/6-31G(d,p) theory is HOMO and 177th molecular orbital is LUMO in the Zn[(I4FPTH)<sub>2</sub>] complex. The transition observed at 479 nm in the TDB3LYP/6-31G(d,p) level consists of mainly HOMO-1 $\leftrightarrow$ LUMO and HOMO $\leftrightarrow$ LUMO+1 and transition assigned at 266 nm is belong to HOMO-17 $\leftrightarrow$ LUMO+1, HOMO-16 $\leftrightarrow$ LUMO, HOMO-

2 $\leftrightarrow$ LUMO+2, HOMO-1 $\leftrightarrow$ LUMO+2, HOMO $\leftrightarrow$ LUMO+3 transitions. The absorption bands for Zn[(I4FPTH)<sub>2</sub>] complex observed at 654, 436 and 259 nm were assigned at 744, 431, 310 nm in the calculation with B3LYP/6-31G(d,p) theory, respectively (Table 6).

In the FTIR spectra of I4FPTH<sub>2</sub> in Table 7, the experimental bands at 3292, 3174 and 3073 cm<sup>-1</sup> correspond to the stretching of  $\nu$ (N6–H26),  $\nu$ (N19–H30), and  $\nu$ (N20–H31) bonds, respectively, whereas  $\nu$ (N6–H) belong to isatin ring and  $\nu$ (N19–H30) belong to thiosemicarbazone group were assigned at 3381 and 3328 cm<sup>-1</sup> for Zn[(I4FPTH)<sub>2</sub>] and at 3405 and 3277 cm<sup>-1</sup> for Ni[(I4FPTH)<sub>2</sub>] complexes, respectively. The  $\nu$ (N6–H26),  $\nu$ (N19–H30) and  $\nu$ (N20–H31) bands stretching of I4FPTH<sub>2</sub> compound have been calculated at 3643, 3502 and 3428 cm<sup>-1</sup> with B3LYP/6–31G(d,p). Whereas in the Zn[(I4FPTH)<sub>2</sub>] complex, the  $\nu$ (N6–H) belong to isatin ring and  $\nu$ (N19–H30) belong to thiosemicarbazone group were assigned at 3648 and 3604 cm<sup>-1</sup>, and assigned at 3653 and 3613 cm<sup>-1</sup> for Ni[(I4FPTH)<sub>2</sub>]. The  $\nu$ (N20–H31) for I4FPTH<sub>2</sub> observed at 3073 cm<sup>-1</sup> was disappeared in Zn[(I4FPTH)<sub>2</sub>] and Ni[(I4FPTH)<sub>2</sub>] complexes, it is assumed that this could be due to the dissociation of the proton. The presence of the band at 1681 cm<sup>-1</sup> in the Zn(II) complex agrees with the uncoordinated nature of the CO group, whereas CO group of I4FPTH<sub>2</sub> assigned at 1684 cm<sup>-1</sup> undergoes a negative shift for Ni[(I4FPTH)<sub>2</sub>] complex. This indicates coordination also occurs via C=O functional groups in addition to C=N and C=S functional groups.

#### 4. CONCLUSIONS

Results of quantum chemical calculations of 1H-indole 2,3-dione-3-(N-4-fluorophenyl) thiosemicarbazone and its Zinc (II) and Nickel (II) complexes showed that HOMO energies and polarizability of complexes are found higher than those ligand. In addition to quantum chemical calculations, experimental values indicates that Zn(II) complex of ligand coordinates via C=N and C=S of its ligand while Ni(II) complex coordinates via C=O C=N and C=S. The results of <sup>13</sup>C NMR calculation with B3LYP/6-311G(2d,2p) method were obtained most sensitive in the all methods.

#### ACKNOWLEDGEMENTS

Authors thank to Nigde University Scientific Research Projects Unit (NUBAP, Project Number: FEB 2011/01) and Kastamonu University KÜBAP-01/2013-31 for their financial support during this study.

#### REFERENCES

1. Sriram D, Yogeeswari P, Gopal G. Synthesis, Anti-HIV and Antitubercular Activities of Lamivudine Prodrugs. European Journal of Medicinal Chemistry. 2005;40(12):1373–1376.



2. Pandeya SN, Sriram D, Nath G, DeClercq E. Synthesis, Antibacterial, Antifungal and Anti-HIV Activities of Schiff and Mannich Bases Derived from Isatin Derivatives and N-[4-(4-Chlorophenyl)thiazole-2-yl]thiosemicarbazide. *European Journal of Pharmaceutical Sciences*. 1999;9(1):25–31.
3. Pirrung MC, Pansare SV, Das Sarma K, Keith KA, Kern ER. Combinatorial Optimization of Isatin- $\beta$ -thiosemicarbazone as Anti-poxvirus Agents. *Journal of Medicinal Chemistry*. 2005;48 (8):3045–3050.
4. Bal TR, Anand B, Yogeeswari P, Sriram D. Synthesis and Evaluation of Anti-HIV Activity of Isatin  $\beta$ -thiosemicarbazone Derivatives. *Bioorganic & Medicinal Chemistry Letters*. 2005;15 (20):4451–4455.
5. Sriram D, Perumal Y. Towards the Design and Development of Agents with Broad Spectrum Chemotherapeutic Properties for the Effective Treatment of HIV/AIDS. *Current Medicinal Chemistry*. 2003;10(17):1689–1695.
6. Pirrung MC, Pansare SV, Das Sarma K, Keith KA, Kern ER. Combinatorial Optimization of Isatin- $\beta$ -thiosemicarbazones as Anti-poxvirus Agents. *Journal of Medicinal Chemistry*. 2005;48(8):3045-3050.
7. Bal TR, Anand B, Yogeeswari P, Sriram D. Synthesis and Evaluation of Anti-HIV Activity of Isatin  $\beta$ -thiosemicarbazone Derivatives. *Bioorganic & Medicinal Chemistry Letters* 2005;15(20):4451-4455.
8. Karalı N, Terzioğlu N, Gursöy A. Synthesis and Structure–Activity Relationships of 3-Hydrazono-1H-2-Indolines with Antituberculosis Activity. *Arzneimittel Forschung-Drug Research*. 1998;48(7):758-763.
9. Sriram D, Yogeeswari P, Gopal G. Synthesis, Anti-HIV and Antitubercular Activities of Lamivudine Prodrugs. *European Journal of Medicinal Chemistry*, 2005;40(12):1373-1376.
10. Pandeya SN, Sriram D, Nath G, De Clercq E. Synthesis, Antibacterial, Antifungal and Anti-HIV Evaluation of Schiff and Mannich Bases of Isatin and Its Derivatives with Triazole. *Arzneimittel Forschung-Drug Research*. 2000;50(1):55-59.
11. Kandemirli F, Arslan T, Karadayı N, Ebenso EE, Köksoy B. Synthesis and Theoretical Study of 5-Methoxyisatin-3-(N-cyclohexyl)-Thiosemicarbazone and its Ni(II) and Zn(II) Complexes. *Journal of Molecular Structure*. 2009;938(1-3):89-96.
12. Kandemirli F, Arslan T, Koksoy B, Yılmaz M. Synthesis, Characterization and Theoretical Calculations of 5-Methoxyisatin-3-Thiosemicarbazone Derivatives. *Journal of the Chemical Society of Pakistan*. 2009;31(3):498-504.
13. Kandemirli F, Koksoy B, Arslan T, Sağdıç S, Berber H. Synthesis and Theoretical Study of Bis(fluoroisatinato)mercury(II). *Journal of Molecular Structure*. 2009;921(1-3):172–177.

14. Gunesdogdu Sagdinc S, Kandemirli F, Köksoy B, Bayari SH. Experimental and Quantum Chemical Studies of 5-Fluoroisatin-3-(N-Cyclohexylthiosemicarbazone) and Its Metal Complexes. *Phosphorus, Sulfur, and Silicon*. 2012;187(10):1243–1260.
15. Gunesdogdu-Sagdinc S, Köksoy B, Kandemirli F, Bayari SH. Theoretical and Spectroscopic Studies of 5-Fluoro-Isatin-3-(N-Benzylthiosemicarbazone) and Its Zinc(II) Complex. *Journal of Molecular Structure*. 2009;917(2):63-70.
16. Karali N, Gürsoy A, Kandemirli F, Shvets N, Kaynak FB, Özbey S, Kovalishyn V, Dimoglo A. Synthesis and Structure-Antituberculosis Activity Relationship of 1H-Indole-2,3-Dione Derivatives. *Bioorganic & Medicinal Chemistry*. 2007;15(17):5888-5904.
17. Kandemirli F, Akkaya Y, Vurdu CD. Synthesis and Quantum Chemical Calculations of 4-(2-Fluorophenyl)-1-(2-Oxoindolin-3-ylidene)thiosemicarbazone and Its Zinc(II) Complexes. *Asian Journal of Chemistry*. 2013;25(17):9722-9730.
18. Kandemirli F, Choudhary M I, Siddiq S, Saracoglu M, Sayiner H, Arslan T, Erbay A, Köksoy B. Quantum Chemistry – Molecules for Innovations, 2012, InTech - Open Access Publisher.
19. Frisch MJ, Trucks GW, Schlegel HB, Scuseria GE, Robb MA, Cheeseman JR, Scalmani G, Barone V, Mennucci B, Petersson GA, Nakatsuji H, Caricato M, Li X, Hratchian HP, Izmaylov AF, Bloino J, Zheng G, Sonnenberg JL, Hada M, Ehara M, Toyota K, Fukuda R, Hasegawa J, Ishida M, Nakajima T, Honda Y, Kitao O, Nakai H, Vreven T, Montgomery JA, Jr Peralta JE, Ogliaro F, Bearpark M, Heyd JJ, Brothers E, Kudin KN, Staroverov VN, Kobayashi R, Normand J, Raghavachari K, Rendell A, Burant JC, Iyengar SS, Tomasi J, Cossi M, Rega N, Millam NJ, Klene M, Knox JE, Cross JB, Bakken V, Adamo C, Jaramillo J, Gomperts R, Stratmann RE, Yazyev O, Austin AJ, Cammi R, Pomelli C, Ochterski JW, Martin RL, Morokuma K, Zakrzewski VG, Voth GA, Salvador P, Dannenberg JJ, Dapprich S, Daniels AD, Farkas Ö, Foresman JB, Ortiz JV, Cioslowski J, Fox D. 2009, Gaussian, Inc, Wallingford CT.

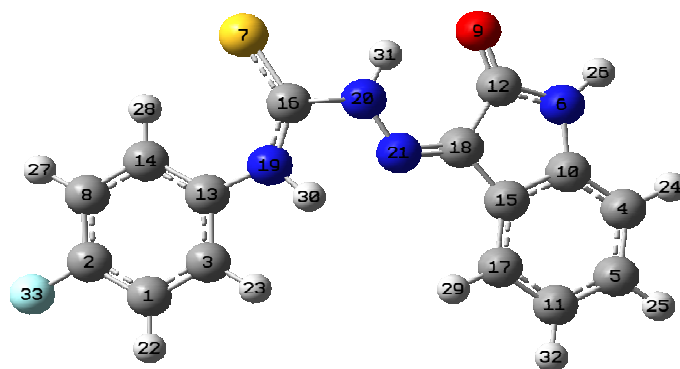


**Figure 1** The optimized structure of 3-(N-4-fluorophenyl)-1H-indole-2,3-dione thiosemicarbazone molecules with the atom numbering calculated by using B3LYP/6-311G(d,p)

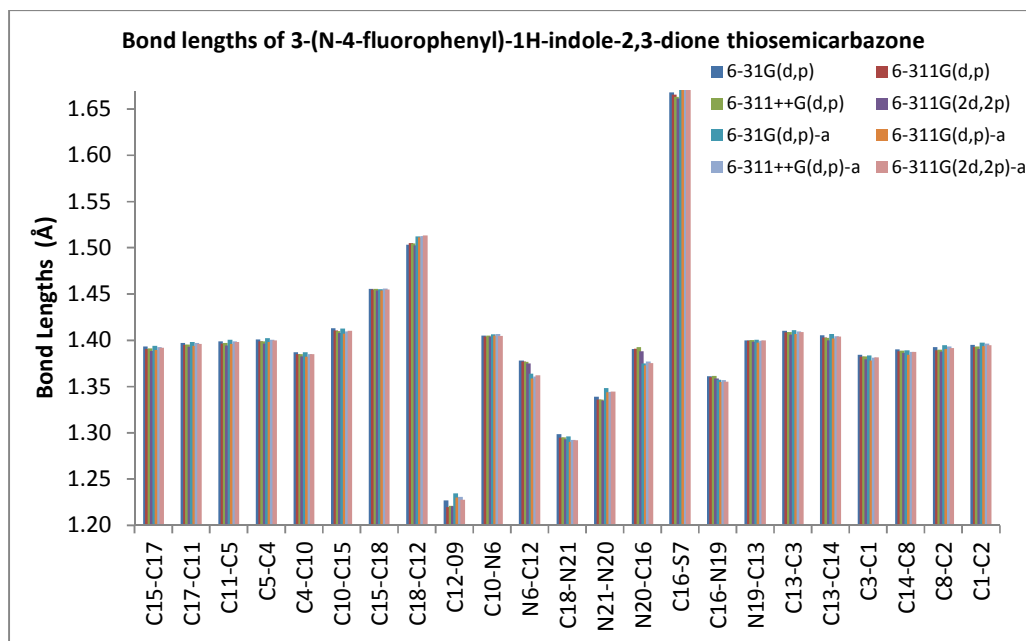


**Figure 2** Bond lengths of 3-(N-4-fluorophenyl)-1H-indole-2,3-dione thiosemicarbazone molecules

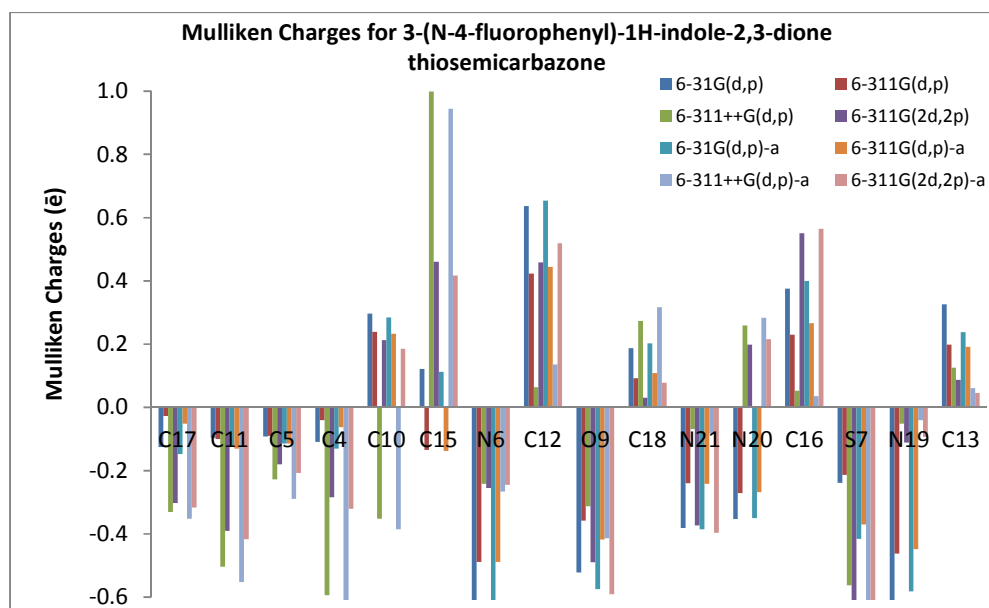
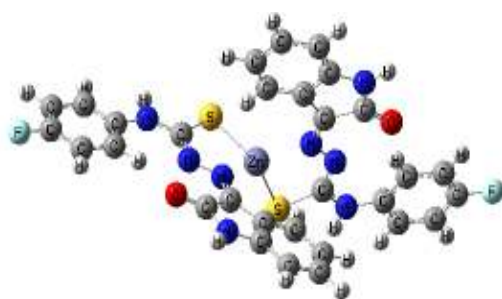
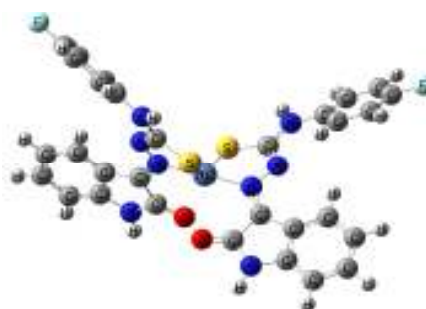


**Figure 3** Mulliken charges of 3-(N-4-fluorophenyl)-1H-indole-2,3-dione thiosemicarbazone molecules



Zn[(I4FPTH)<sub>2</sub>]



Ni[(I4FPTH)<sub>2</sub>]

**Figure 4** Optimized structure of Zn[(I4FPTH)<sub>2</sub>] and Ni[(I4FPTH)<sub>2</sub>]

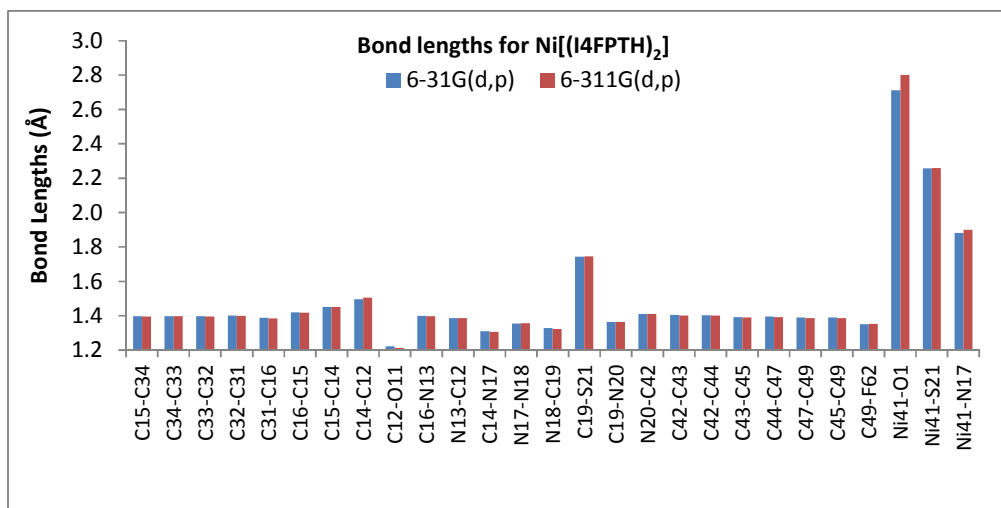
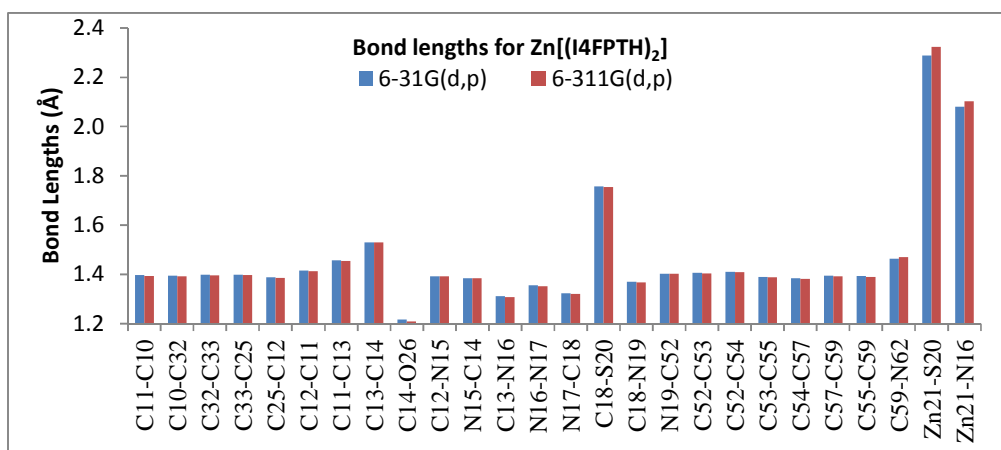


**Figure 5** Bond lengths for (a) Zn[(I4FPTH)<sub>2</sub>] and (b) Ni[(I4FPTH)<sub>2</sub>] complexes

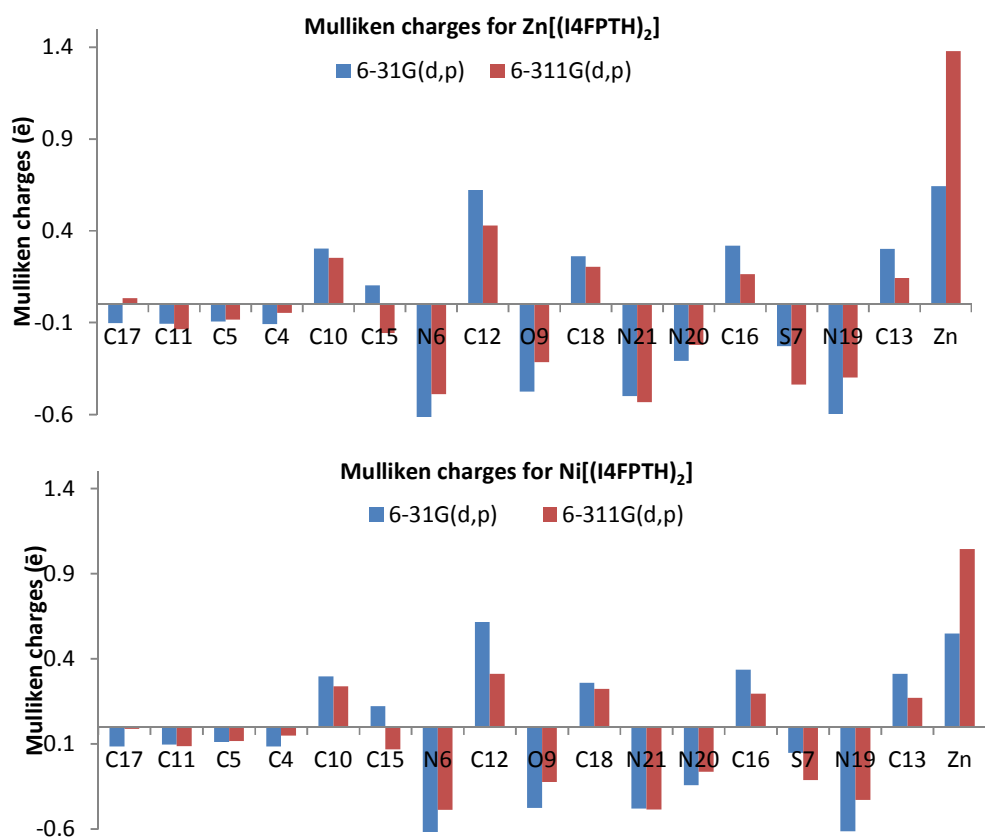


**Figure 6** Mulliken charges for Zn[(I4FPTH)<sub>2</sub>] and Ni[(I4FPTH)<sub>2</sub>] complexes



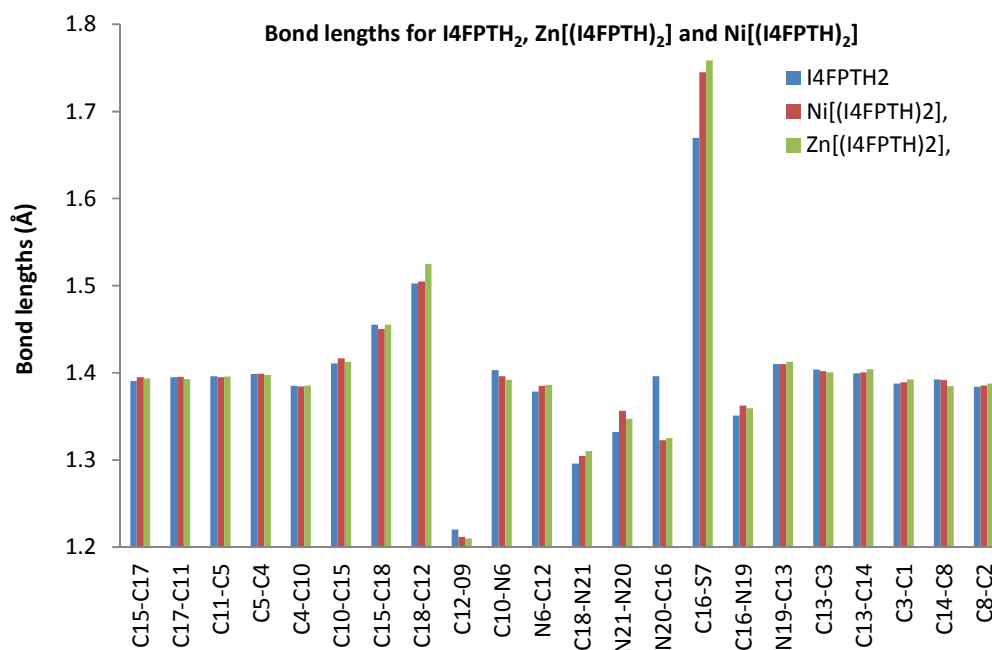


**Figure 7** Bond lengths for I4FPTH<sub>2</sub>, Zn[(I4FPTH)<sub>2</sub>] and Ni[(I4FPTH)<sub>2</sub>] calculated with B3LYP/6-311G(d,p) method

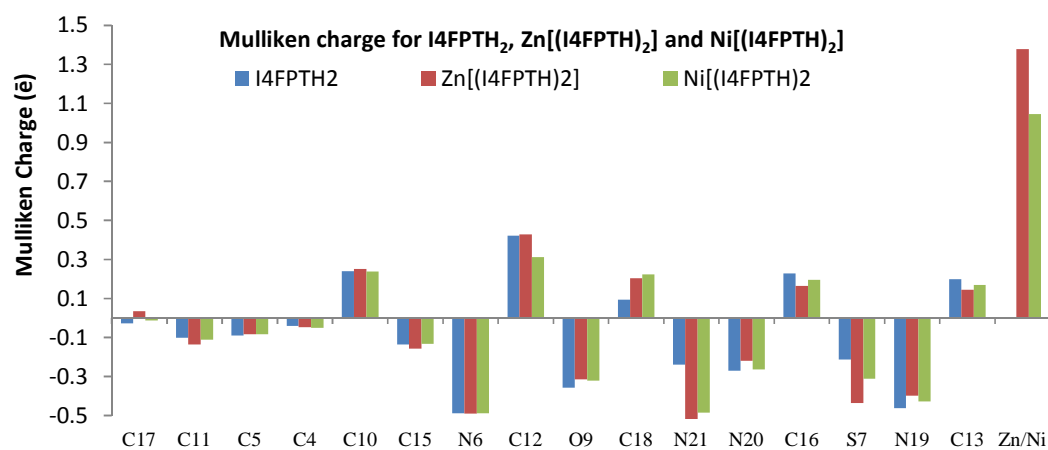


**Figure 8** Mulliken charge for I4FPTH<sub>2</sub>, Zn[(I4FPTH)<sub>2</sub>] and Ni[(I4FPTH)<sub>2</sub>] calculated with B3LYP/6-311G(d,p) method

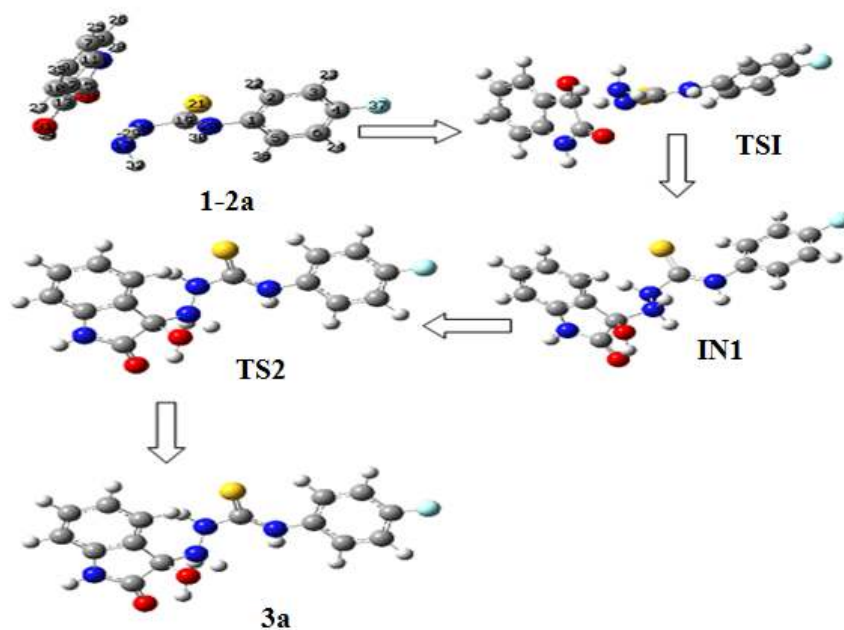


**Figure 9** Optimized structures of Reactants, transition states (TS), intermediates (IN1) and products

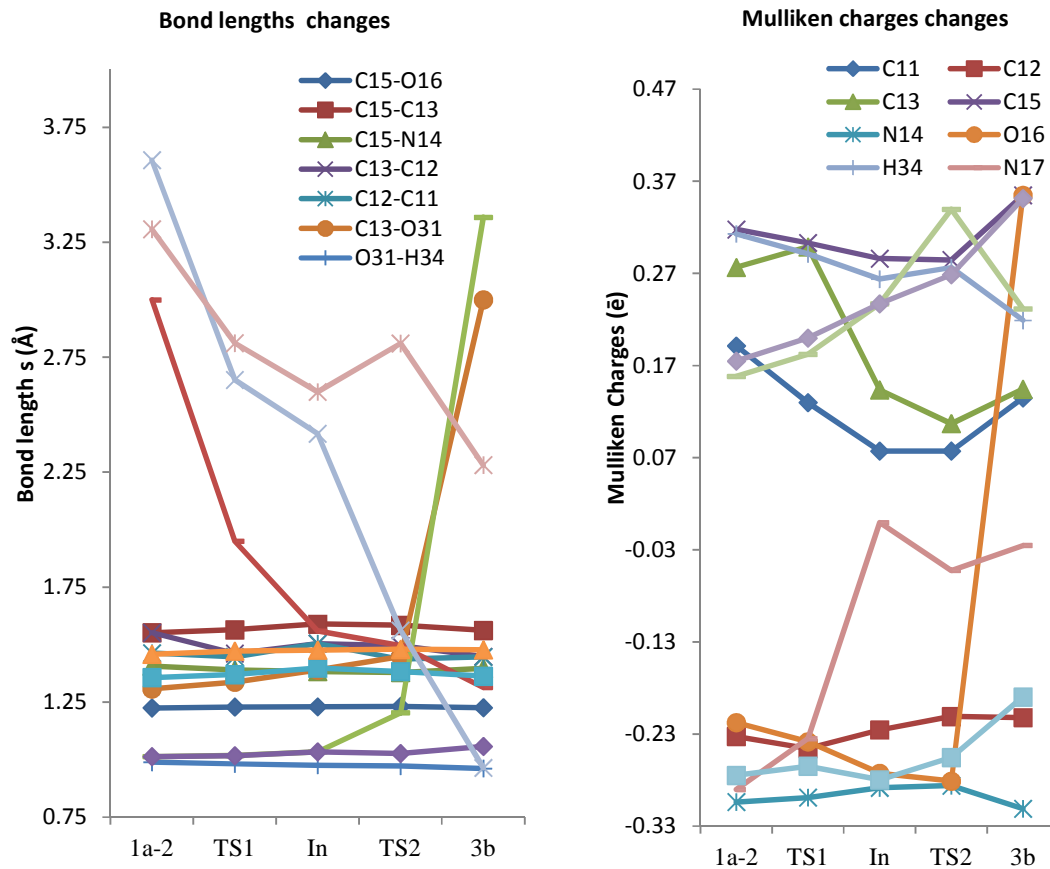


**Figure 10** Bond lengths changes and Mulliken charges changes in the reaction mechanism for 3-(N-4-fluorophenyl)-1H-indole-2,3-dione thiosemicarbazone molecule

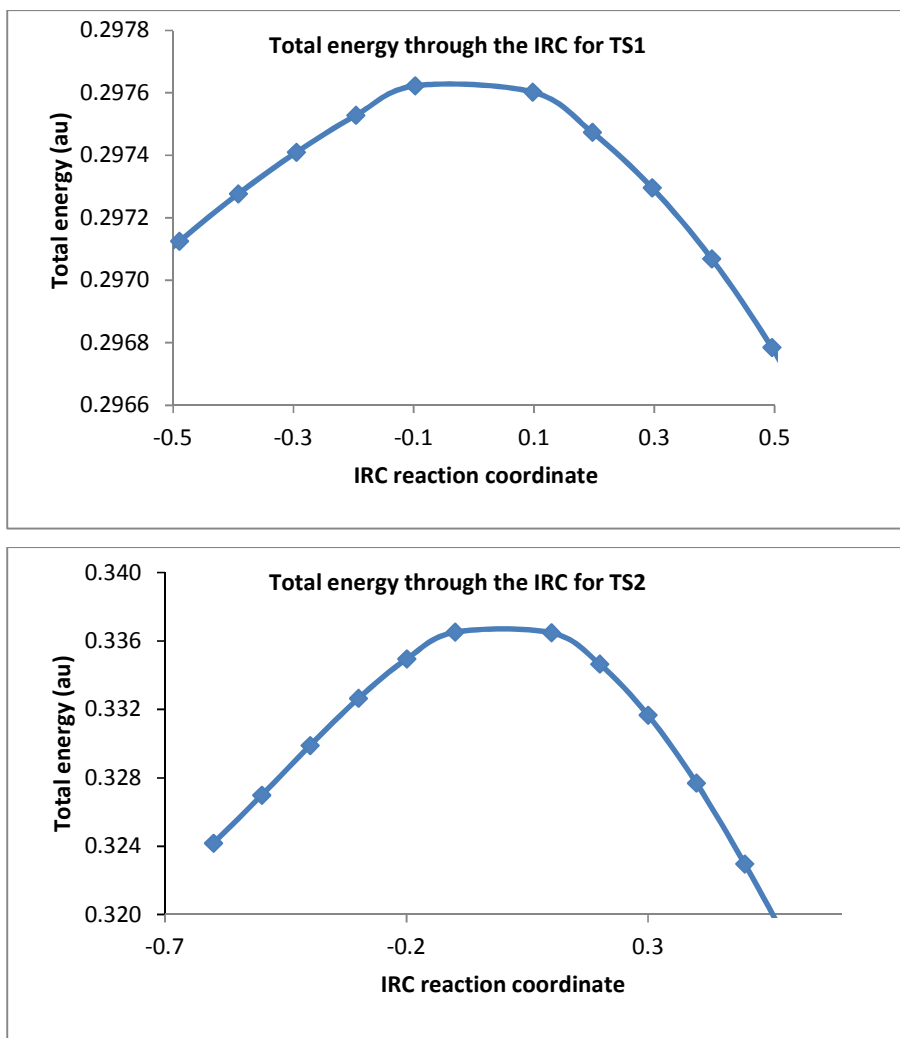


**Figure 11** Total energy through the IRC for 3-(N-4-fluorophenyl)-1H-indole-2,3-dione thiosemicarbazone molecule

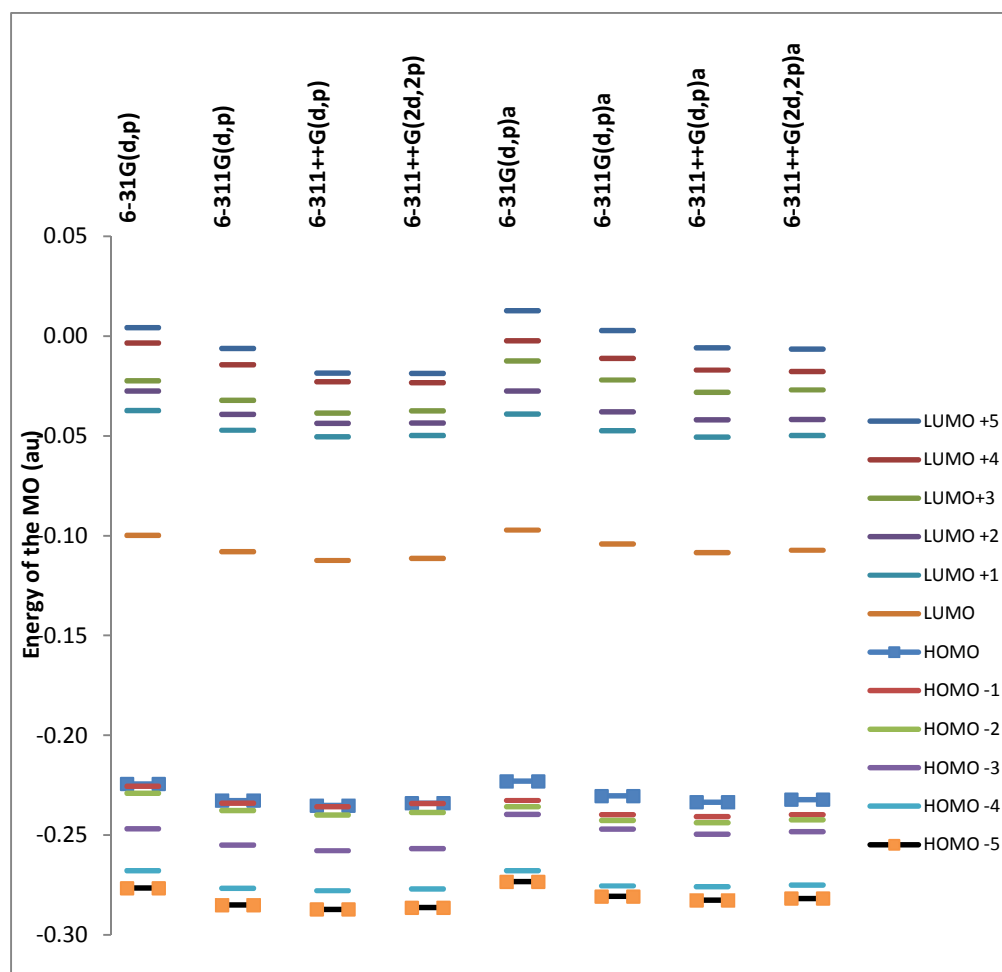


**Figure 12** Molecular orbital energies of 3-(N-4-fluorophenyl)-1H-indole-2,3-dione thiosemicarbazone molecules

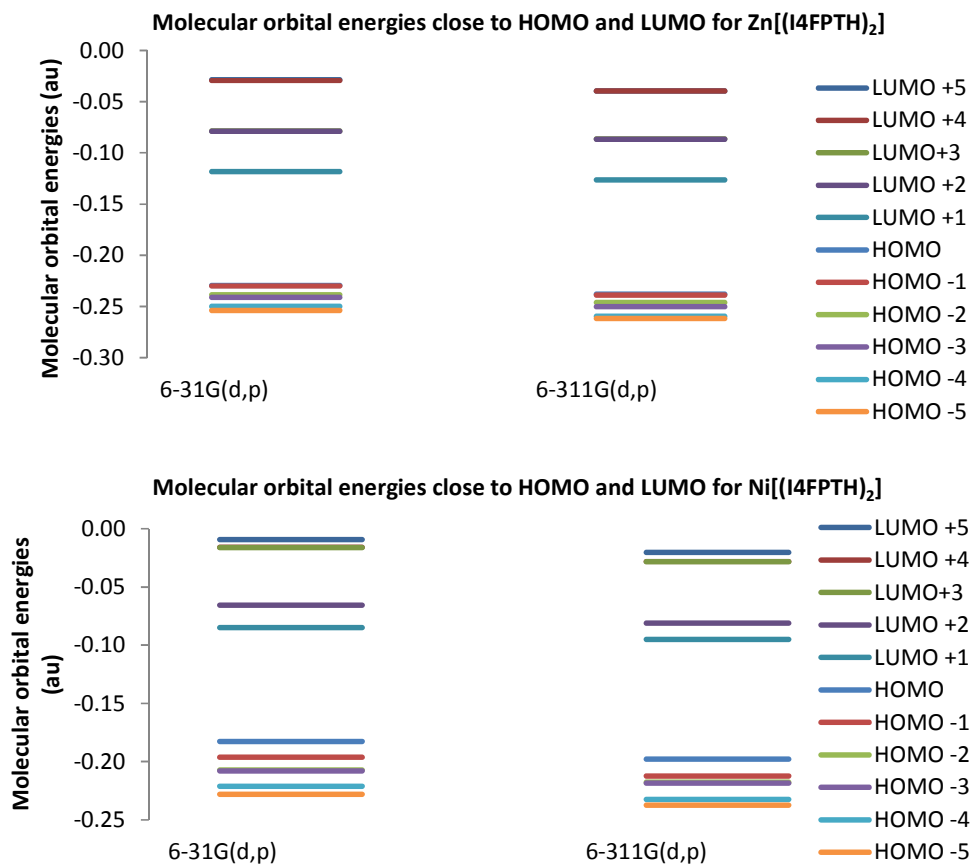


**Figure 13** Molecular orbital energies close to HOMO and LUMO for Zn[(I4FPTH)<sub>2</sub>] and Ni[(I4FPTH)<sub>2</sub>]

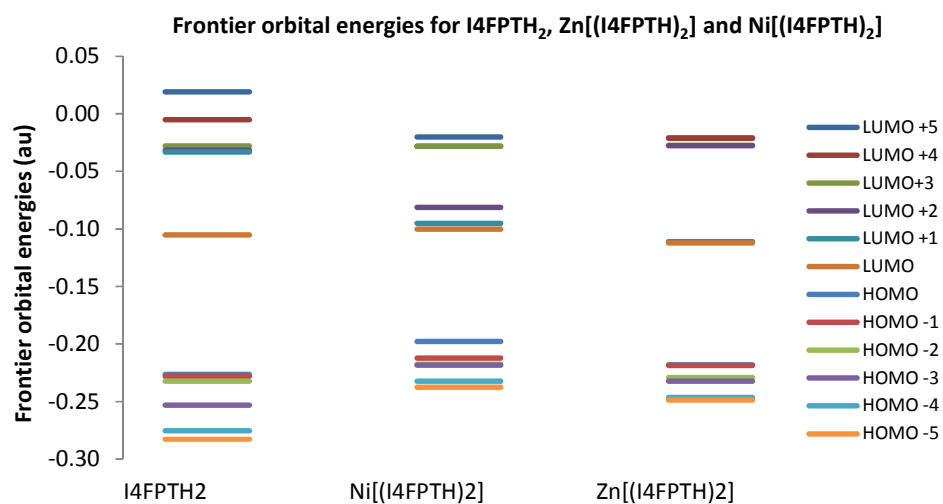


**Figure 14** Frontier orbital energies for I4FPTH<sub>2</sub>, Zn[(I4FPTH)<sub>2</sub>] and Ni[(I4FPTH)<sub>2</sub>] calculated with B3LYP/6-311G(d,p) method



**Table 1. Electronic energies for I4FPTH<sub>2</sub>, Zn[(I4FPTH)<sub>2</sub>] and Ni[(I4FPTH)<sub>2</sub>] complexes**

<b>Compounds</b>		<b>Electronic Energies (B3LYP) (au)</b>			
		<b>6-31G(d,p)</b>	<b>6-311G(d,p)</b>	<b>6-311++G(d,p)</b>	<b>6-311++ G(2d,2p)</b>
I4FPTH <sub>2</sub>	gas	-1370.50690942	-1370.75982233	-1370.77771190	-1370.81055509
	DMSO	-1370.53408912	1370.78639203	-1370.80560437	-1370.83735522
Ni[(I4FPTH) <sub>2</sub> ]	gas	-4248.03385394	4248.66059430		
Zn[(I4FPTH) <sub>2</sub> ]	gas	-4519.01672668	-4519.68637322		

**Table 2. Polarizabilty of I4FPTH<sub>2</sub>, Zn[(I4FPTH)<sub>2</sub>] and Ni[(I4FPTH)<sub>2</sub>]**

Compounds	6-31G(d,p)	6-311G(d,p)	6-311++G(d,p)	6-311++G(2d,2p)
I4FPTH <sub>2</sub>	246.4	257.0	277.5	283.0
Zn[(I4FPTH) <sub>2</sub> ]	542.0	554.8		
Ni[(I4FPTH) <sub>2</sub> ]	552.5	562.4		

**Table 3. Experimental and theoretical <sup>1</sup>H NMR values of 3-(N-4-fluorophenyl)-1H-indole-2,3-dione thiosemicarbazone molecule**

Atoms	Exp.	6-31G(d,p)	6-311G(d,p)	6-311++G(d,p)	6-311G(2d,2p)	6-31G(d,p)-a	6-311G(d,p)-a	6-311++G(d,p)-a	6-311G(2d,2p)-a
H29	7.74	7.66	7.79	7.75	7.93	7.92	8.05	7.91	8.20
H24	6.92	6.72	6.85	6.82	7.00	7.25	7.41	7.19	7.55
H32	7.13	7.14	7.22	7.18	7.38	7.43	7.58	7.41	7.73
H25	7.35	7.34	7.43	7.40	7.62	7.74	7.87	7.71	8.06
H28	7.58	9.89	10.00	9.97	10.32	7.94	9.85	9.66	10.17
H23	7.58	6.72	6.89	6.85	7.11	7.60	7.45	7.33	7.66
H27	7.27	7.07	7.23	7.19	7.39	7.49	7.64	7.53	7.81
H22	7.27	6.97	7.10	7.06	7.29	7.51	7.64	7.53	7.82
H30	10.83	9.41	9.45	9.41	10.04	9.13	9.60	9.70	10.20
H31	11.26	12.59	12.36	12.33	13.11	13.03	12.63	12.56	13.29
H26	11.26	6.22	6.25	6.21	6.77	8.17	8.24	8.36	8.76
R <sup>2</sup>		0.856	0.861	0.864	0.888	0.773	0.841	0.870	0.870

**Table 4. Experimental and theoretical <sup>13</sup>C NMR values of 3-(N-4-fluorophenyl)-1H-indole-2,3-dione thiosemicarbazone molecule**

Atoms	Exp.	6-31G(d,p)	6-311G(d,p)	6-311++G(d,p)	6-311G(2d,2p)	6-31G(d,p)-a	6-311G(d,p)-a	6-311++G(d,p)-a	6-311G(2d,2p)-a
C17	122	116	125	125	125	118	111	128	127
C11	128	118	127	127	128	119	112	131	129
C5	133	125	136	136	136	128	121	140	140
C4	111	105	113	113	114	108	101	118	117
C10	142	136	147	147	148	139	132	151	151
C15	128	117	127	127	128	116	109	127	127
C18	132	123	131	131	131	131	124	139	138
C12	161	154	164	164	167	157	150	171	171
C16	177	169	179	179	181	175	168	184	182
C13	135	129	141	141	142	130	122	144	143
C3	121	115	124	124	124	124	117	129	128
C14	120	115	124	124	125	127	120	125	125
C1	115	111	120	120	120	112	105	124	123
C8	115	112	121	121	121	112	105	122	121
C2	163	155	169	169	169	158	151	171	170
R <sup>2</sup>		0.987	0.984	0.984	0.985	0.950	0.941	0.983	0.985

**Table 5. Experimental and theoretical  $^1\text{H}$  NMR and  $^{13}\text{C}$  NMR values of  $\text{Zn}[(\text{I4FPTH})_2]$  complex**

$^1\text{H}$ NMR				$^{13}\text{C}$ NMR			
Atoms	Exp.	6-31G(d,p)	6-311G(d,p)	Atoms	Exp.	6-31G(d,p)	6-311G(d,p)
H28	6.96	6.52	6.60	C17	127.8	120	130
H24	7.70	7.66	7.74	C31	131.3	116	126
H27	7.32	6.72	6.76	C5	131.5	127	137
H25	7.60	7.13	7.22	C4	111.7	104	112
H29	6.98	6.61	6.86	C10	131.7	136	147
H23	7.77	10.25	10.33	C15	131.3	116	124
H28	7.62	7.30	7.40	C18	132.1	139	148
H22	7.51	6.92	7.05	C12	136.3	151	161
H30	10.96	6.95	7.30	C16	166.6	172	181
H26	10.42	6.19	6.16	C13	131.6	130	141
				C3	129.6	121	130
				C1	122.8	113	122
				C8	117.2	110	119
				C2	142.7	155	169

**Table 6. Oscillator strengths (f) and excitation energies (eV) for UV spectra values calculated with TDB3LYP and TDB3LYP**

<b>I4FPTH<sub>2</sub></b>										
<b>B3LYP</b>									<b>bp86 cep-31g*</b>	
<b>Exp(nm)</b>	<b>6-31G(d,p)</b>		<b>6-311G(d,p)</b>		<b>6-311++G(d,p)</b>		<b>6-311++G(2d,2p)</b>			
371	356	3.47(0.46)	357	3.47(0.46)	362	3.43(0.45)	362	3.42(0.45)E4	338	3.68(0.40)
257	256	4.85(0.23)	259	4.78(0.23)	262	4.72(0.19)	263	4.71(0.18)	243	4.71(0.26)
<b>B3LYP</b>										
<b>Zn[(I4FPTH)<sub>2</sub>]</b>					<b>Ni[(I4FPTH)<sub>2</sub>]</b>					
<b>Exp(nm)</b>	<b>6-31G(d,p)</b>		<b>6-311G(d,p)</b>		<b>Exp(nm)</b>	<b>6-31G(d,p)</b>		<b>6-311G(d,p)</b>		
368	479	2.59(0.26)E3	484	2.56(0.30)E3	654	744	1.66(0.08)	664	1.87(0.06)E3	
256	266	4.66(0.22)E32	267	4.64(0.22)	436	431	2.87(0.22)	432	2.87(0.19)E12	
					259	310	3.99(0.10)	305	4.05(0.08)E35	

**Table 7. Experimental and theoretical the FTIR spectra of I4FPTH<sub>2</sub>, Zn[(I4FPTH)<sub>2</sub>] and Ni[(I4FPTH)<sub>2</sub>]**

<b>Experimental</b>	<b><math>\nu(\text{N6-H26})</math></b>	<b><math>\nu(\text{N19-H30})</math></b>	<b><math>\nu(\text{N20-H31})</math></b>	<b><math>\nu(\text{C=O})</math></b>	<b><math>\nu(\text{C=N})</math></b>	<b><math>\nu(\text{C-S})</math></b>
I4FPTH <sub>2</sub>	3292	3174	3073	1684	1586	835
Zn[(I4FPTH) <sub>2</sub> ]	3381	3328	-	1681	1575	810
Ni[(I4FPTH) <sub>2</sub> ]	3405	3277	-	1660	1576	812
<b>Theoretical 6-311G(d,p)</b>						
I4FPTH <sub>2</sub>	3643	3502	3428	1776	1621	958
Zn[(I4FPTH) <sub>2</sub> ]	3648	3604	-	1793	1591	820
Ni[(I4FPTH) <sub>2</sub> ]	3653	3613	-	1791	1630	833